from which it is clear that the relaxation rates are variational maxima of the right-hand side, that is, eigenvalues of the matrix $\boldsymbol{M}$. Modes are the eignevectors of $\boldsymbol{M}$.

The weights, a_i, of each mode in general require knowledge of the eigenvectors of $\boldsymbol{M}$. For the relaxation modulus defined by

$$\sum_{i=1}^{(N-1)} \frac{\langle \rho_{i\alpha}\rho_{i\beta}\rangle}{s_i} = [(N-1) + (\lambda_\alpha{}^2 - 1)G(t)]\delta_{\alpha\beta} \quad \text{(B.6)}$$

with

$$G(t) = \sum_{i=1}^{(N-1)} w_i e^{-\mu_i t} \quad \text{(B.7)}$$

then since

$$\frac{\langle \rho_{i\alpha}\rho_{i\beta}\rangle}{s_i} = \delta_{\alpha\beta}[\lambda_\alpha{}^2 + (1-\lambda_\alpha{}^2)\mu t M_{ii} + O(t^2)]$$

and $\sum_{i=1}^{(N-1)} M_{ii} = \sum_{(i=1}^{(N-1)} \mu_i$, we have $w_i = 1$.

Finally we therefore have that a mode approximation to the relaxation gives

$$G(t) = \sum_{i=1}^{(N-1)} e^{-\mu_i t} \quad \text{(B.8)}$$

where μ_i are eigenvalues of $\boldsymbol{M}$ defined by (B.2).

References and Notes

(1) Yamamoto, M. *J. Phys. Soc. Jpn.* **1956**, *11*, 433.
(2) Lodge, A. S. *Trans. Faraday Soc.* **1956**, *52*, 120.
(3) (a) Wilson, A. D.; Prosser, H. J. *Developments in Ionic Polymers*; Applied Science Publishers: New York, London, 1983; Vol. 1. (b) Peiffer, D. G.; Kaladas, J.; Duvdevani, I.; Higgins, J. S. *Macromolecules* **1987**, *20*, 1397.
(4) de Gennes, P.-G. *J. Chem. Phys.* **1971**, *55*, 572.
(5) Slater, G. W.; Noolandi, J. *Biopolymers* **1986**, *25*, 431.
(6) Rouse, P. E. *J. Chem. Phys.* **1953**, *21*, 1273.
(7) Zimm, B. H. *J. Chem. Phys.* **1956**, *24*, 269.
(8) Doi, M.; Edwards, S. F. *J. Chem. Soc., Faraday Trans. 2* **1978**, *74*, 1789, 1802.
(9) Roitman, D.; Zimm, B. H. *J. Chem. Phys.* **1984**, *81*, 6333.
(10) Doi, M.; Edwards, S. F. *The Theory of Polymer Dynamics*; Clarendon Press: Oxford, 1986.
(11) Verdier, P. H.; Stockmayer, W. H. *J. Chem. Phys.* **1962**, *36*, 227.
(12) Cates, M. E. *Macromolecules* **1987**, *20*, 2289.
(13) Gonzalez, A. E. *Polymer* **1984**, *25*, 1469.
(14) Flory, P. J. *Trans. Faraday Soc.* **1960**, *56*, 772.
(15) Fricker, H. S. *Proc. R. Soc. London A* **1973**, *335*, 269.

Theory of Thermoreversible Gelation

Fumihiko Tanaka

Laboratory of Physics, Faculty of General Education, Tokyo University of Agriculture and Technology, Fuchu-shi, Tokyo 183, Japan.

Received June 6, 1988; Revised Manuscript Received September 20, 1988

ABSTRACT: A simple model is introduced to describe observed coexistence of gelation and phase demixing in atactic polystyrene solutions. Our theory demonstrates that the multiple-equilibria conditions for molecular clustering caused by physical cross-linking can describe the characteristic features of the temperature–concentration phase diagram. Detailed calculations are made for the concentration dependence of the gelation curve, the spinodal curve, the mean cluster size, and the osmotic pressure under the assumption that intracluster association is negligible. Effect of molecular weight and functionality is examined. Our results show reasonable agreement with experimental data obtained for atactic polystyrene in carbon disulfide. The condition for the gelation line to pass over the critical demixing point is clarified.

1. Introduction

Since the discovery[1] that certain chemically inactive atactic polystyrene (at-PS) solutions can exhibit gelation, there has been a growing interest[2-6] in the phenomena of physical gelation. Recent experimental studies[2,3] have furnished strong evidence that the gelation is thermally reversible and a fairly universal phenomenon that takes place in a wide variety of solvents. Although the origin of associative interchain interaction has not been clarified, the binding energy connecting a pair of polymer segments is expected to be of the order of thermal energy, so that bonding–unbonding equilibrium is easily attained. The current understanding of the experimental observations is based on the co-occurrence[2] of sol–gel transition and two-phase separation on the temperature–concentration phase diagram. Effect of the molecular weight of at-PS and of solvent species has been examined[2,3] in detail. Although quantitatively different, the essential characteristics of the phase behavior are found to be preserved regardless of these substitutions.

Only few attempts have been made to develop theories that would describe such phase behavior, and they are highly qualitative. For example, de Gennes[7] presented an overall picture about the competition between gelation and segregation in some polymeric solutions. As the molecular origin of the phase behavior was not sufficiently elucidated in this study, neither the precise position of the phase boundary nor any solution properties were calculated.

Coniglio et al.[8] proposed a microscopic model on the basis of the original classic ideas of gelation developed by Flory[9-11] and Stockmayer.[12] Though there were some findings on the relationship between the gelation line and the coexistence curve, it was impossible to relate a model parameter p (percolation probability) with the solute concentration without ambiguity. Hence, they did not calculate physical quantities, such as mean cluster size or osmotic pressure, *as a function of the concentration*.

Some computer simulations[13] were attempted in relation to the lattice percolation theory. Because the molecular basis of the percolation model is not clear, difficulty remains in interpreting the model parameters in terms of the system quantities on which the real solution will depend.

Although these researches have thrown much useful light on many aspects of the general problem, it is the purpose of this paper to establish a microscopic foundation for the study of associating solutions and to give a complete picture to the important case of thermoreversible gelation.

We start with the lattice theory of polydisperse solutions originally developed by Flory[14,15] and Huggins[16] and in-

0024-9297/89/2222-1988$01.50/0

corpolate the idea of specific interaction capable of forming interchain bridges. We then derive the cluster distribution function and estimate the values of observable quantities under the assumption that intracluster association is negligible. Finally, we compare the results with the experimental observation for at-PS/CS_2.

2. The Cluster Distribution Function

Consider a system of identical molecules, each carrying f (≥ 2) identical functional groups and dissolved in a solvent. The functional groups on a molecule are assumed to be identical for simplicity and capable of forming physical bonds by pairwise association. The potential barrier of the cross-linking considered here is of the order of thermal energy, so that bonding–unbonding equilibrium is easily attained by thermal activation. One may include by the term "molecule" various types of reactive objects such as functional monomeric units, long flexible chains with active side groups, rigid rodlike molecules carrying specific parts capable of association, and so on.

In thermal equilibrium, intermolecular reaction yields polydisperse molecular aggregates, which we call "cluster" in the following. We derive in this section the size distribution of such clusters. Starting from the lattice theory of polymer solutions developed by Flory[14,15] and Huggins,[16] we incorporate the statistics of random polycondensation[12] into the theory.

Let a^3 be the volume of a solvent molecule, and let na^3 be the volume of an f functional molecule. Each functional molecule is considered to be composed of n elementary units, whose volume is assumed to be comparable to the solvent volume. We then divide the system volume V into small cells of size a. The total number of the cells is given by $\Omega \equiv V/a^3$. Let N_0 be the number of solvent molecules in the system, and let N_m ($m = 1, 2, 3, ...$) be the number of clusters in which m functional molecules are connected by bonds. Hereafter, we refer to the clusters as unimer ($m = 1$), dimer ($m = 2$), trimer ($m = 3$), etc. The total number of functional molecules is given by $N = \sum_{m=1}^{\infty} mN_m$. We assume that each lattice cell is occupied by either a solvent molecule or an elementary unit on a functional molecule, so that space-filling condition $\Omega = N_0 + nN$ is satisfied.

In terms of these definitions the volume fraction of each component is given by $\phi_0 = N_0/\Omega$ for the solvent, and $\phi_m = mnN_m/\Omega$ for the m cluster. We have the total concentration ϕ of the solute molecules by the sum

$$\phi = \sum_{m=1}^{\infty} \phi_m \tag{2.1}$$

The equilibrium weight distribution of the clusters can be described by $w_m \equiv \phi_m/\phi$.

The free energy of our system may be constructed from two terms

$$F = F_{rea} + \Delta F_{mix} \tag{2.2}$$

by the consideration of the two processes starting from the reference state, in which pure solvent and pure unreacted molecules are prepared separately. Here, F_{rea} is the free energy change required to form the clusters from the reference state by connecting in a pairwise fashion the functional groups. It may be written as

$$F_{rea} = \sum_{m=1}^{\infty} N_m \mu_m^0 \tag{2.3}$$

in terms of the chemical potential μ_m^0, or equivalently the internal free energy, of a single isolated m cluster.

The second term ΔF_{mix} describes the free energy change in the process of mixing thus constructed clusters with the solvent. According to the lattice theory of Flory–Huggins type, it is given by

$$\beta \Delta F_{mix} = N_0 \ln \phi_0 + \sum_{m=1}^{\infty} N_m \ln \phi_m + \Omega \chi \phi (1 - \phi) \tag{2.4}$$

where $\beta \equiv 1/k_B T$ is the inverse temperature and χ the solvent–solute interaction parameter.

Following the standard procedure, we take derivatives of the free energy with respect to the number of molecules of each kind and find the corresponding chemical potentials

$$\beta \mu_0 = \beta \mu_0^0 + \ln (1 - \phi) + (1 - 1/\langle m \rangle n)\phi + \chi \phi^2 \tag{2.5a}$$

$$\beta \mu_m = \beta \mu_m^0 + \ln \phi_m - (mn - 1) + mn(1 - 1/\langle m \rangle n)\phi + mn\chi(1 - \phi)^2 \tag{2.5b}$$

where

$$\langle m \rangle \equiv \phi / (\sum_{m=1}^{\infty} \phi_m/m) \tag{2.6}$$

is the number-averaged mean cluster size.

In thermal equilibrium, each molecule is in chemical equilibrium through bonding and unbonding processes. This imposes the following multiple-equilibria conditions:

$$\mu_m/m = \text{independent of } m \quad (\text{and therefore equals } \mu_1) \tag{2.7}$$

Substitution of (2.5b) for μ_m yields

$$\phi_m = K_m \phi_1^m \tag{2.8}$$

for the volume fraction of m clusters, where the association constant K_m is given by

$$K_m = \exp(m - 1 - \Delta_m) \tag{2.9}$$

in terms of the reduced free energy difference Δ_m defined by

$$\Delta_m \equiv \beta(\mu_m^0 - m\mu_1^0) \tag{2.10}$$

The free energy gain per single functional molecule by participating in an m cluster from isolation is given by $\delta_m = \Delta_m/m$.

3. Micellization and Gelation

It has been shown that the free energies Δ_m of cluster formation determine the entire distribution of aggregates. The total concentration is now given by a power series of ϕ_1, the unimer concentration, the mth power of which is accompanied with coefficient K_m. Application of the Cauchy–Hadamard's theorem gives the convergence radius Φ of the power series in the form

$$1/\Phi = \overline{\lim_{m \to \infty}} (K_m)^{1/m} = e^{1-\delta_\infty} \tag{3.1}$$

where the least upper bound of the limit has been indicated by a bar. The quantity δ_∞ is the limiting value of δ_m as $m \to \infty$, i.e. the free energy gain per molecule for the formation of an infinite (macroscopic) cluster.

Within the radius of convergence, eq 2.1 gives a one-to-one relationship between ϕ and ϕ_1. By inverting this relation, we express the unimer concentration in terms of the total concentration:

$$\phi_1 = \psi(\phi) \qquad \text{for} \quad 0 \leq \phi_1 \leq \Phi \tag{3.2}$$

The function $\psi(\phi)$ is a monotonically increasing function of ϕ since all the coefficients K_m in (2.1) are positive definite.

Several cases are conceivable. Figure 1 schematically shows the exponent $\delta_m + 1/m - 1$ of $K_m^{-1/m}$ as a function of m. Since we are treating solute molecules capable of

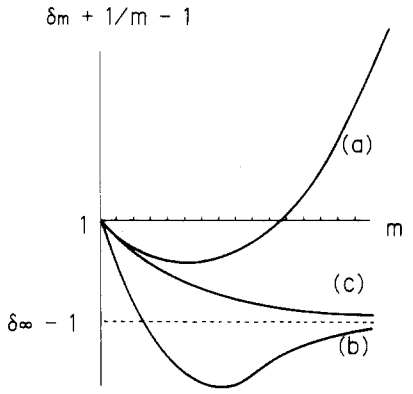

Figure 1. Exponent $\delta_m + 1/m - 1$ shown as a function of the cluster size m. It either takes a minimum at finite m (a, b) or monotonically decreases to a finite value (c).

clustering, the function must either take a minimum at a certain finite m (parts a and b of Figure 1) or decrease monotonically to a finite value $\delta_\infty - 1$ (Figure 1c).

Let m_0 be the value of m at which the curve reaches minimum, including $m_0 = \infty$ for the monotonic case. It should satisfy the condition

$$\frac{\partial}{\partial m}(\delta_m + 1/m - 1) = 0 \tag{3.3}$$

We next find the cluster size m at which fraction ϕ_m becomes maximum for a given ϕ_1. Equation 2.8 gives the condition for ϕ_m to be maximum as

$$\partial\Delta_m/\partial m = 1 + \ln \phi_1 \tag{3.4}$$

Let m^* be the value satisfying this condition. Since ϕ_m should not exceed unity by definition, the unimer concentration ϕ_1 is limited from above by the inequality $K_{m^*}(\phi_1)^{m^*} \leq 1$, and hence

$$\phi_1 \leq \phi_1^* \equiv \exp(\delta_{m^*} + 1/m^* - 1) \tag{3.5}$$

In the case where m^* is finite, the upper bound in (3.5) is called "critical micelle concentration (cmc)" in the literature,[17,18] since, near below this value, contribution from the finite clusters (micelles) amounts to a finite fraction of the total concentration ϕ. Sharpness in the appearance of the clusters is controlled by the curvature of the function $\delta_m + 1/m - 1$ around m^*. At cmc, the condition (3.4) reduces to (3.3), and hence we have $m_0 = m^*$.

In the case where m^* is infinite, on the other hand, a macroscopic cluster appears as soon as ϕ_1 exceeds the critical value:

$$\phi_1^* \equiv e^{\delta_\infty - 1} \tag{3.6}$$

Hence, we have gelation. The total concentration ϕ^* obtained from ϕ_1^* gives the concentration at which sol-to-gel transition occurs. It depends on the temperature through δ_∞. For ϕ above ϕ^*, the summation of the power series on the right-hand side of (2.1) cannot reach ϕ, since it does not include the contribution from the infinite cluster. The amount $\phi - \sum\phi_m$ of shortage in the normalization in fact gives the volume fraction of the generated gel component.

We now proceed to study the number-averaged mean cluster size. Within the radius of convergence, the denominator in (2.6) is transformed to

$$\sum_{m=1}^{\infty} \frac{K_m}{m}\phi_1{}^m = \int_0^{\phi_1}\left(\sum_{m=1}^{\infty} K_m\phi_1{}^{m-1}\right) d\phi_1 = \int_0^{\phi_1}\frac{\phi}{\phi_1}\, d\phi_1 = \int_0^{\phi}\frac{\phi}{\psi(\phi)}\psi'(\phi)\, d\phi \tag{3.7}$$

where we have used the relation (3.2).

Let us denote as $\kappa(\phi)$ the function appearing in the integrand

$$\kappa(\phi) \equiv \phi\frac{d}{d\phi}\ln\psi(\phi) \tag{3.8}$$

In terms of this function, the mean cluster size is given by:

$$\langle m\rangle = \phi/\int_0^{\phi}\kappa(\phi)\, d\phi \tag{3.9}$$

This function $\kappa(\phi)$ plays an essential role in the development of our theory.

Although it is straightforward to include finite m^*, we focus hereafter in this paper our attention on the case of infinite m^* to describe physical gelation.

4. Solution Properties below the Gelation Concentration

We next study the change of solution properties associated with cluster formation. The total concentration is limited to the range below the gelation transition in this section. Attention is especially paid on the concentration dependence of the physical quantities.

Let us first consider the osmotic pressure π. Thermodynamic argument[15] derives a general relationship between the osmotic pressure and the solvent chemical potential: $\pi = -\Delta\mu_0/a^3$, where $\Delta\mu_0 \equiv \mu_0 - \mu_0{}^0$. Hence, we have

$$-\pi\beta a^3 = \ln(1-\phi) + \phi - \frac{1}{n}\int_0^{\phi}\kappa(\phi)\, d\phi + \chi\phi^2 \tag{4.1}$$

for $\phi < \phi^*$, where we have explicitly used the function κ defined by (3.9). In dilute regime we can expand this function in powers of the concentration:

$$\kappa(\phi) = 1 + \kappa_1\phi + \kappa_2\phi^2 + \ldots \tag{4.2}$$

Substitution of (4.2) into (4.1) yields the dimensionless second virial coefficient in a simple form:

$$\tilde{A}_2 = \tfrac{1}{2} - \chi + \frac{\kappa_1}{2n} \tag{4.3}$$

As we will show in the following, the coefficient κ_1 is always negative, so that the value of $\tilde{A}_2$ is reduced by cluster formation as it should.

We next consider phase separation. As the temperature is lowered, the system becomes metastable against concentration fluctuations and the free energy is lowered when the system is separated into two phases of different concentration.[15] Let ϕ' and ϕ'' be the higher and the lower concentration of the coexisting two phase, respectively. The condition for the two phases to be in thermal equilibrium is given by $\mu_m(\phi') = \mu_m(\phi'')$ for $m = 1, 2, 3, \ldots$ Due to the multiple-equilibria conditions (2.7), however, these reduce to a single one:

$$\mu_1(\phi') = \mu_1(\phi'') \tag{4.4}$$

Finally, we consider thermodynamic instability of the system against concentration fluctuations. Because the condition for a two-component system to be stable requires the inequality $\partial\Delta\mu_0/\partial\phi < 0$, the line separating the unstable region on the temperature–concentration plane is determined by the equation $\partial\Delta\mu_0/\partial\phi = 0$. The line is called the "spinodal line". Equation 4.1 gives

$$\frac{1}{1-\phi} + \frac{\kappa(\phi)}{n\phi} - 2\chi = 0 \tag{4.5}$$

Comparison with the original Flory–Huggins theory clearly shows that the deviation of $\kappa(\phi)$ from unity gives the effect of intermolecular association.

The critical demixing point of the solution is obtained by imposing the two conditions (4.4) and (4.5) simultaneously, or equivalently, $\partial\Delta\mu_0/\partial\phi = \partial^2\Delta\mu_0/\partial\phi^2 = 0$. Hence, we have

$$\frac{1}{(1-\phi)^2} + \frac{\kappa'(\phi)\phi - \kappa(\phi)}{n\phi^2} = 0 \tag{4.6}$$

in combination with (4.5) for the critical point. Therefore, one can easily be convinced that proper combination of the system parameters such as functionality, reaction energy, or molecular volume can make the gelation line pass onto the critical point. Such an interesting situation is realized when the three conditions (3.6), (4.5), and (4.6) are simultaneously satisfied. As the concentration fluctuations accompanying a sol–gel transition and those associated with the critical demixing point belong to quite different universality classes, the competition between them is expected to appear in this particular case. Many questions related to this phenomenon remain open.

5. Inclusion of Postgel Properties

So far we have confined ourselves to the discussion of the pregel region, where the total solute concentration is smaller than ϕ^*. As soon as ϕ exceeds ϕ^*, a three-dimensional network comprised of an infinite number of molecules appears. This is gel formation.

Let ϕ_G be the volume fraction occupied by the gel. Since the infinite sum (2.1) does not contain the gel component, we must set

$$\phi_S = \sum_{m=1}^{\infty} \phi_m \tag{5.1}$$

for $\phi > \phi^*$, where ϕ_S shows the volume fraction of the polymer contained in the sol phase. The fraction ϕ_S, when combined with the polymer volume fraction in the gel phase ϕ_G, satisfies the correct normalization:

$$\phi_S + \phi_G = \phi \tag{5.2}$$

In a similar way the number-averaged mean cluster size $\langle m \rangle$, which appears in the chemical potentials, must be interpreted as the one for the sol component. Hence, we have

$$\beta\mu_m = \beta\mu_m{}^0 + \ln \phi_m - (mn - 1) + mn\phi - \frac{m}{\langle m \rangle}\phi_S + mn\chi(1-\phi)^2 \tag{5.3}$$

To study postgel properties, we now regard our system as a three-component system composed of solvent, sol, and gel. For the system to attain equilibrium, we require overall uniformity of the single-molecular chemical potential. The chemical potential μ_G for a molecule participating in the gel network can be found by taking the macroscopic limit: $\mu_G = \lim_{m\to\infty} (\mu_m/m)$. Equation 5.3 yields

$$\beta\mu_G = \beta\mu_1{}^0 + \delta_\infty - n(1-\phi) - \frac{\phi_S}{\langle m \rangle} + \chi n(1-\phi)^2 \tag{5.4}$$

where use has been made of the definition (2.10) for δ_m. Note that the translational entropy $\ln(\phi_\infty)$ has dropped out, as the gel is macroscopic.

We can readily confirm this result in a quite different way. The free energy for mixing the three components can be expressed as

$$\beta\Delta F_{mix} = N_0 \ln \phi_0 + \sum_{m=1}^{\infty} N_m \ln \phi_m + N_G \ln \phi_G + \Omega\chi\phi(1-\phi) \tag{5.5}$$

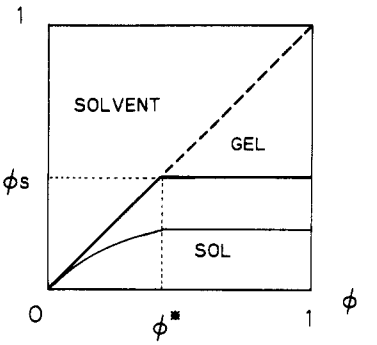

Figure 2. Relative amount of three components (solvent, sol, and gel) shown as a function of the total concentration. The sol fraction is constant above the gelation threshold. The unimer concentration ϕ_1 is indicated by a thin line.

where $\Omega \equiv N_0 + \sum mN_m + m^*N_G$ is the total volume of the system, N_G the number of gel clusters, and m^* the number of molecules in a single infinite cluster. After taking the derivatives with respect to N_0, N_m, and N_G, we set $N_G = 1$ and $m^* \to \infty$. We find exactly the same results as in (5.3) and (5.4).

In addition to the multiple-equilibria conditions, we now impose an extra conditions: $\mu_G = \mu_1$. Combination of (5.3) and (5.4) yields

$$\phi_1 = e^{\delta_\infty - 1} \qquad \text{for any} \quad \phi > \phi^* \tag{5.6}$$

The unimer concentration remains constant at critical value $\phi_1{}^*$ above the threshold, while the total concentration ϕ is increased. As ϕ_1 determines the cluster distribution function in the sol component, it is evident that the average cluster size $\langle m \rangle$ also remains constant above the gelation threshold. The excess amount $\phi - \phi_S$ is absorbed into the infinite network without modifying the composition in the sol phase. Results of our discussion are summarized in Figure 2.

This conclusion is an agreement with the picture proposed by Stockmayer[12] but in disagreement with the postgel picture suggested by Flory.[9-11] Since the internal inconsistency of Flory's argument was pointed by Stockmayer[12] in detail, we do not refer to it any further here.

6. Application of the Stockmayer Distribution

In this section an attempt is made to obtain quantitative description of thermoreversible gelation. We first consider how the internal free energy $\mu_m{}^0$ of a cluster is constructed.

Let $Z_m \equiv \exp(-\beta\mu_m{}^0)$ be the partition function of a single cluster in the solution. Principles of statistical mechanics then give

$$Z_m = \frac{W_m(f)}{m!} p^{m-1}(1-p)^{fm-2m+2} \tag{6.1}$$

where p is the probability of bond formation for a pair of active groups and $W_m(f)$ the number of combinations in which m molecules may form an m cluster. It has been tacitly assumed for simplicity that intramolecular cross-linking is excluded, so that we have $m - 1$ bonds and $fm - 2m + 2$ unbonded functional groups. The combinatorial factor depends on the structure of a molecule and is given[12] by

$$W_m(f) = \frac{(fm-m)!f^m}{(fm-2m+2)!} \tag{6.2}$$

provided that the f functional groups on a molecule are indistinguishable. For a long flexible chain carrying a large number of active side groups, the functionality f is of the order of n, the degree of polymerization, and the factor f^m in W_m must be omitted since the side groups can be se-

quentially numbered. The probability distribution (6.1) combined with (6.2) is called the Stockmayer distribution as it was first derived by him.[12]

The free energy gain Δ_m for polycondensation can be written as

$$e^{-\Delta_m} = Z_m/(Z_1)^m = \frac{(fm-m)!f^m}{m!(fm-2m+2)!}\left(\frac{p}{(1-p)^2}\right)^{m-1} \tag{6.3}$$

The statistical weight of a bond formation relative to the weight of two unreacted functionalities is expressed by

$$\frac{p}{(1-p)^2} = e^{-\beta\Delta f_0} \tag{6.4}$$

according to the law of mass action, where Δf_0 is the free energy of a single bond formation. The association constant $K_m = \exp(m - 1 - \Delta_m)$ can readily be derived from (6.3).

The function $\delta_m + 1/m - 1$ is a monotonically decreasing function as it should and approaches a finite value

$$\delta_\infty - 1 = -\ln\lambda - (f-1)\ln(f-1) + (f-2)\ln(f-2) \tag{6.5}$$

as $m \to \infty$, where the parameter λ is defined by:

$$\lambda \equiv \frac{efp}{(1-p)^2} \tag{6.6}$$

Let us proceed to sum up the power series in (2.1) and obtain the function $\psi(\phi)$, and hence $\kappa(\phi)$, of our most concern. Let $x \equiv \lambda\phi_1$ and $y \equiv \lambda\phi$ be the reduced concentration of unimers and of the total solute molecules, where λ is a temperature shift factor defined by (6.6). We then find

$$y = fS_0(x) = \frac{\alpha(1-f\alpha/2)}{(1-\alpha)^2} \tag{6.7}$$

within the radius of convergence. Here, a new parameter α has been introduced by the definition

$$x \equiv \alpha(1-\alpha)^{f-2} \tag{6.8}$$

A series of functions $S_i(x)$ ($i = 0, 1, 2, \ldots$) are defined by

$$S_i(x) \equiv \sum_{m=1}^{\infty} \frac{m^i(fm-m)!}{m!(fm-2m+2)!}x^m \tag{6.9}$$

Stockmayer[12] provided a general prescription for summing these series, and we have applied it to obtain (6.7). The radius of convergence of these power series is given by $x_c = (f-2)^{f-2}/(f-1)^{f-1}$ or $\alpha_c = 1/(f-1)$. Hence, we have $\phi_1^* = x_c/\lambda$. This can be rewritten as $\phi_1^* = \exp(\delta_\infty - 1)$ as it should from the general argument leading to (3.6). As the function y takes the value $1/(2(f-2))$ at criticality $\alpha = \alpha_c$, the total concentration ϕ^* at which gel starts to appear is given by

$$\phi^* = 1/(2(f-2)\lambda) \tag{6.10}$$

This relation between concentration and temperature shift factor determines the sol–gel transition curve on the temperature–concentration plane.

In order to obtain the function $\psi(\phi)$, let us first solve (6.7) and express the parameter α in terms of y. Substituting the result into (6.8), we find

$$\psi(y) = \frac{\{1+2y-(1-2(f-2)y)^{1/2}\}\{f-1+(1-2(f-2)y)^{1/2}\}^{f-2}}{(f+2y)^{f-1}} \tag{6.11}$$

and hence

$$\kappa(y) = \frac{y}{(1-2(f-2)y)^{1/2}}\left(\frac{f-2+2(1-2(f-2)y)^{1/2}}{1+2y-(1-2(f-2)y)^{1/2}} - \frac{(f-2)^2}{f-1+(1-2(f-2)y)^{1/2}}\right) - \frac{2(f-1)y}{f+2y} \tag{6.12}$$

We have now reached a complete solution of the problem of thermoreversible gelation under the assumption that intracluster association is negligible. Any physical quantity can readily be calculated from the function $\kappa(y)$ according to the general method developed in the preceding sections.

From the coefficient $\kappa_1 = -\{(f-2)^2 + 4f^2(f-1)\}/2f$ in the linear term of $\kappa(y)$, for example, we have

$$\tilde{A}_2 = \tfrac{1}{2} - \chi - \frac{\lambda}{4nf}\{(f-2)^2 + 4f^2(f-1)\} \tag{6.13}$$

for the second virial coefficient. It is negative at the temperature $T = \Theta$, where $\chi(\Theta) = {}^1/_2$. This temperature is the Θ temperature[15] of the solution composed of the same solvent and the solute of the inactive counterparts (i.e. molecule of the same species but with no functional groups on it).

Average cluster size is obtained from

$$\langle m\rangle = y/\int_0^y \kappa(y)\,dy \tag{6.14}$$

In the next section results of detailed numerical calculations will be shown on the osmotic pressure, the mean cluster size, the gelation line, and the spinodal line.

7. Results of Numerical Calculations and Comparison with the Experiments

To develop our analysis a step further and to compare it with experimental observations, we split the free energy Δf_0 of bonding into two parts

$$\beta\Delta f_0 = \beta\Delta\epsilon - \Delta s/k_B \tag{7.1}$$

where $\Delta\epsilon$ (<0) and Δs are energy and entropy change, respectively, required for a bond formation. We then have

$$\lambda = \lambda_0 e^{-\beta\Delta\epsilon} \tag{7.2}$$

by the use of the amplitude λ_0 defined by $\lambda_0 \equiv f\exp(1 + \Delta s/k_B)$.

Let us introduce the reduced temperature τ by the definition $\tau \equiv 1 - \Theta/T$, where Θ is the temperature. For T near the Θ temperature, the Flory interaction parameter χ is known[15] to obey in most cases the formula

$$\chi = \tfrac{1}{2} - \psi_1\tau \tag{7.3}$$

Here, an amplitude ψ_1 takes a numerical value of order unity, the precise value of which is dependent on the solvent–solute combination. In terms of the reduced temperature, $\beta\Delta\epsilon$ can be rewritten as

$$\beta\Delta\epsilon = -r(1-\tau) \tag{7.4}$$

where $r \equiv -\Delta\epsilon/k_B\Theta$ (>0) is the dimensionless bonding energy measured relative to the thermal energy.

We have five parameters specifying chemical constituents of the system: f, functionality of a molecule; n, real volume of a molecule; λ_0, parameter related to the entropy of bond formation; r, bonding energy/thermal energy; ψ_1, solvent–solute interaction.

Let us first examine the effect of the bonding free energy. Since the condition for gel formation (6.10) gives logarithmic dependence of τ on ϕ^*

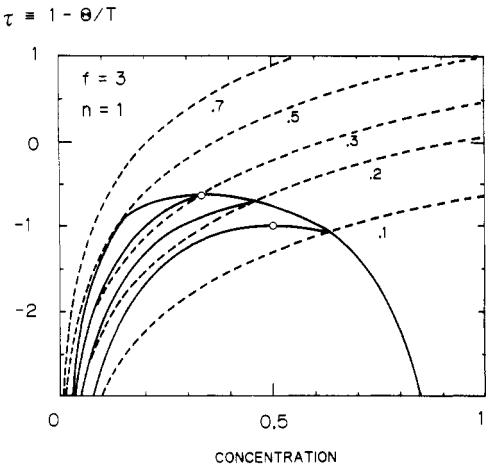

Figure 3. Phase diagram for low molecular weight molecules ($f = 3$, $n = 1$) shown on the plane of reduced temperature τ and volume fraction ϕ: spinodal curves (thick lines), gelation lines (broken lines), critical demixing points (O). Parameter λ_0 is varied from curve to curve.

$$\tau = 1 + \frac{1}{r} \ln (2(f-2)\lambda_0) + \frac{1}{r} \ln \phi^* \qquad (7.5)$$

it is evident that larger r gives slower variation of the gelation line. The line is bound from above by a finite value $\tau(\phi^* = 1) = 1 + (\ln 2(f-2)\lambda_0)/r$, and hence it shifts downward when either r is increased or λ_0 is decreased.

Figure 3 shows a typical example of the phase behavior of functional molecules of low molecular weight ($n = 1$). Gelation and spinodal curves are shown. The critical demixing points are indicated by O. We have set $f = 3$, $\psi_1 = 1$, and $r = 1$ for the numerical calculation. The parameter λ_0 is varied from curve to curve. For smaller values of λ_0 the gelation curve meets with the high-concentration branch of a spinodal curve. Near the intersection, the spinodal region is distorted. The whole plane is divided into four regions: one-phase sol, one-phase gel (clear gel), two-phase sol, and two-phase gel (turbid gel). The intersection moves toward the lower concentration region as λ_0 is increased and passes the critical demixing point at certain value of λ_0. In this figure it occurs at λ_0 between 0.1 and 0.2. As λ_0 increases, the critical point disappears and the higher and the lower branches of a spinodal meet with finite angle, as typically shown in the case of $\lambda_0 = 0.2$. With further increase of λ_0, the gelation line shifts further and a new critical point starts to appear in the postgel region above the gelation line. This occurs at $\lambda_0 = 0.3$. The gelation line has eventually a common tangent at $\lambda_0 = 0.5$ with the low-concentration branch of a spinodal curve. For λ_0 larger than 0.5, the unstable region below the spinodal curve is completely contained in the postgel region. Because the function $\kappa(\phi)$ is fixed at the threshold value $(f-1)/2(f-2)$ in this region, spinodals are independent of λ_0 for $\lambda_0 > 0.5$.

We have qualitatively similar phase diagrams for larger values of the functionality. The whole picture merely shifts toward the dilute region by a small amount.

In Figure 4, the osmotic pressure (divided by the total concentration) together with the number-averaged mean cluster size is plotted as a function of the concentration. The parameter has been chosen as in Figure 3. The reduced temperature is changed from curve to curve. On each thick curve showing the osmotic pressure, spinodal point and gelation point are indicated by O and ●, respectively. Because thermally unstable states cannot exist in equilibrium, the predicted behaviors in the spinodal region are plotted by dotted lines. Though continuous, the derivatives of the osmotic pressure with respect to the

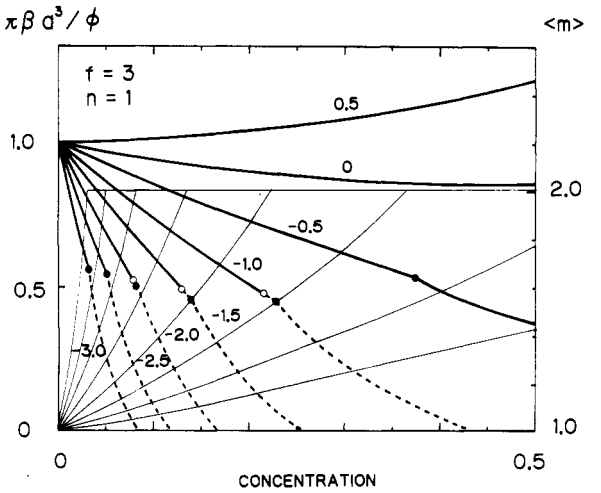

Figure 4. Osmotic pressure (thick lines) and mean cluster size (thin lines) plotted against volume fraction for $n = 1$, $f = 3$, and $\lambda_0 = 0.3$: critical points (O), gelation points (●). Calculated values in the unstable region are indicated by broken lines.

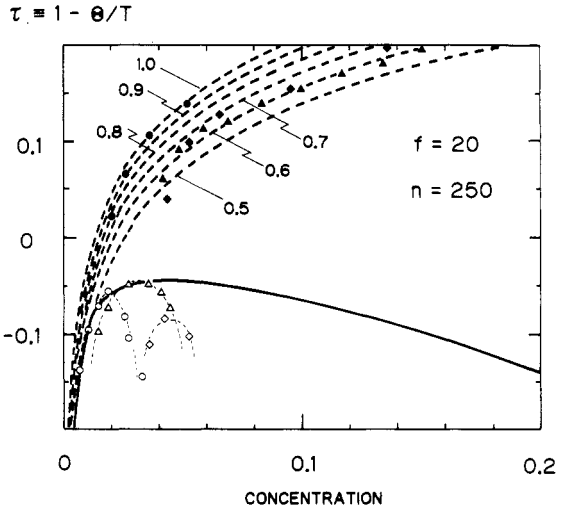

Figure 5. Temperature–concentration phase diagram for $n = 250$ and $f = 20$ shown together with the experimental data obtained for at-PS/CS_2. The weight concentration is translated into the volume concentration by using $\rho = 1.05$ g/cm^3. The solid line shows the calculated spinodal boundary, and the broken lines show the gelation thresholds. The parameter λ_0 is varied from 0.5×10^{-4} to 1.0×10^{-4} to fit the observed data on the sol–gel transition points. Experimental data are indicated by ● ($\bar{M}_n = 2.53 \times 10^5$), ▲ ($\bar{M}_n = 9.06 \times 10^4$), and ● ($\bar{M}_n = 9.15 \times 10^4$).

concentration jumps at gelation points. It should be noted that the initial slope of the curve for $\tau = 0$ is negative, showing that the second virial coefficient does not vanish at $T = \Theta$. The thin lines in this figure show $\langle m \rangle$, the number-averaged mean cluster size. They are constant above the gelation threshold.

We next study the case of long flexible chains. As molecular weight of at-PS studied in the experiments[2] was varied over the range from 9.06×10^4 to 2.65×10^5, the corresponding number of statistical units is estimated as of the order of several hundreds. As the detailed information on the χ parameter is not available for at-PS/CS_2, we have used the value $\psi_1 = 1.05$ for at-PS/cyclohexane in the following calculation.

Figure 5 shows the obtained phase diagram for $n = 250$ and $f = 20$ together with the experimental data.[2] The entropy parameter λ_0 is varied from curve to curve. The volume fraction ϕ can readily be transformed to the weight concentration c by the relation $c = \rho\phi$, where ρ is the density of PS (=1.05 g/cm^3). The result is insensitive to

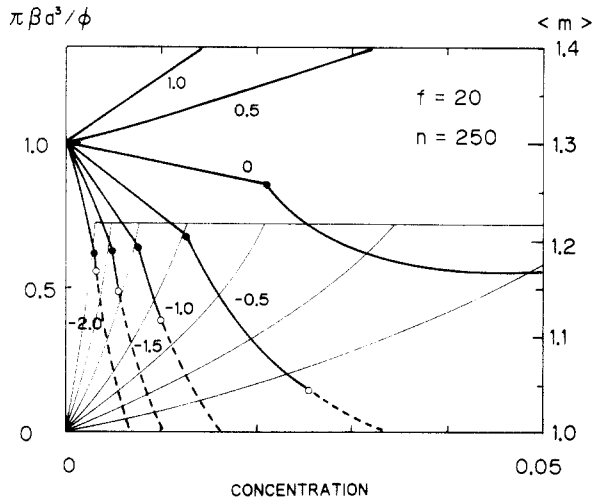

Figure 6. Osmotic pressure and mean cluster size are shown for $n = 250$, $f = 20$, and $\lambda_0 = 0.6 \times 10^{-4}$.

the change of f. For $f = 50$, for example, results can be superposed with this figure by adjusting λ_0. Therefore, there is no reason to consider that particular segments fixed on an at-PS chain participate in the appearance of attractive interaction capable of forming bonds.

To produce an observed slow rate of increase in the gelation line, higher values of r are required. The experimental curve for the CS_2 solvent is properly described by the value $r = 10$ and $\lambda_0 = (0.5\text{–}1.0) \times 10^{-4}$. In fact r was found[2] to vary from 5 to 15 by melting heat measurements.

The osmotic pressure and mean cluster size are shown in Figure 6 for $n = 250$, $f = 20$, and $\lambda_0 = 0.6 \times 10^{-4}$.

8. Discussion

The microscopic theory presented in this paper and interpretation of the calculations based on it are profitable for the understanding of the observed characteristics of thermoreversible gelation. The picture we have presented here provides a starting point to further the study of the nature of this phenomenon. Major points of interest are as follow.

Our theory is severely limited by failure to account for cyclic structures formed by intracluster cross-linkings. As far as irreversible polycondensation of functional units is concerned, considerable investigation has been in fact formulated to improve this shortcoming. For example, Jacobson and Stockmayer[19] presented a complete solution of this problem in a very limited case where functionality f of reacting units is 2, and hence only rings of various sizes can appear by intramolecular reaction. Several revisions of our theory along this line are straightforward and now in progress.

The picture presented in this paper is based on the lattice theory of polydisperse polymeric solution developed by Flory and Huggins. It is a mean field theory and does not correctly predict the nature of concentration fluctuations near the phase transition point. There are two major transitions in our system: gelation and phase separation, each accompanied with their own critical phenomena. Recent investigations strongly suggest that the sol–gel transition belongs to a universal class represented by percolation transition,[13] while critical demixing points of two-component mixtures belong to a universal class of an Ising type ferromagnet.[20] In a special case where the two transitions come close to each other on the temperature–concentration plane, as was pointed out above, fluctuations of a different nature must conflict. Assignment of the region near the confluent point to each critical phenomenon will be of major interest. The ideal case might be realizable experimentally if the combination of the molecular weight of at-PS and the chemical species of the solvent were judiciously chosen.

Our theory can be applicable to the important cases in which clusters of finite size are stabilized.[17,18] Micelles formed amphiphilic molecules or chains[21,22] are typical examples of this case. All thermodynamic properties can be obtained from the general scheme presented here, once the internal structure of each cluster is clarified.

Calculations of dynamical properties such as viscoelasticity, shear-rate dependence of the solution viscosity, or diffusion constant are beyond the scope of this study. As far as the steady-flow viscosity is concerned, however, the cluster distribution function obtained in this way might be applicable for the study of concentration dependence, provided one can estimate the hydrodynamic radius of each cluster from its internal structure. We have analyzed[23] along this line the observed stationary zero-shear viscosity of associating polymers such as metal-sulfonated polystyrene in the solvent of low polarity.

Comprehension of the connection between molecular association and thermodynamic properties is an obvious prerequisite for interpretation of a wide variety of structure formation in macromolecular solutions.

Registry No. Polystyrene, 9003-53-6.

References and Notes

(1) Wellinghoff, S.; Shaw, J.; Baer, E. *Macromolecules* **1979**, *12*, 932.
(2) Tan, T. M.; Moet, A.; Hiltner, A.; Baer, E. *Macromolecules* **1983**, *16*, 28.
(3) Boyer, R. F.; Baer, E.; Hiltner, A. *Macromolecules* **1985**, *18*, 427.
(4) Gan, J. Y. S.; François, J.; Guenet, J. M. *Macromolecules* **1986**, *19*, 173.
(5) Koltisko, B.; Keller, A.; Litt, M.; Baer, E.; Hiltner, A. *Macromolecules* **1986**, *19*, 1207.
(6) Jelich, L. M.; Nunes, S. P.; Paul, E.; Wolf, B. A. *Macromolecules* **1987**, *20*, 1943; 1948; 1952.
(7) de Gennes, P.-G., In *Scaling Concepts in Polymer Physics*; Cornell University Press: New York, 1979; Chapter V.
(8) Coniglio, A.; Stanley, H. E.; Klein, W. *Phys. Rev.* **1982**, *B25*, 6805.
(9) Flory, P. J. *J. Am. Chem. Soc.* **1941**, *63*, 3083; 3091; 3096.
(10) Flory, P. J. *Faraday Discuss. Chem. Soc.* **1974**, *57*, 7.
(11) Flory, P. J. In *Principles of Polymer Chemistry*; Cornell University Press: New York, 1953; Chapter 9.
(12) Stockmayer, W. H. *J. Chem. Phys.* **1943**, *11*, 45; **1944**, *12*, 125.
(13) Stauffer, D.; Coniglio, A.; Adam, M. *Adv. Polym. Sci.* **1982**, *44*, 103.
(14) Flory, P. J. *J. Chem. Phys.* **1942**, *10*, 51; **1944**, *12*, 425.
(15) Flory, P. J. Reference 11; Chapters 12 and 13.
(16) Huggins, M. L. *J. Phys. Chem.* **1942**, *46*, 151.
(17) Tanford, C. *Hydrophobic Effect*; Wiley: New York, 1979.
(18) Israelachvili, J. N. In *Physics of Amphiphiles: Micelles, Vesicles and Microemulsions*; Degiorgio, V., Corti, M., Eds.; North-Holland: Amsterdam, The Netherlands, 1985; p 24.
(19) Jacobson, H.; Stockmayer, W. H. *J. Chem. Phys.* **1950**, *18*, 1600.
(20) de Gennes, P.-G. Reference 7; Chapter IV.
(21) Cates, M. E.; Witten, T. A. *Macromolecules* **1986**, *19*, 732.
(22) Bug, A. L. R.; Cates, M. E.; Safran, S. A.; Witten, T. A. *J. Chem. Phys.* **1987**, *87*, 1824.
(23) Tanaka, F. *Macromolecules* **1988**, *21*, 2189.